

Article

# Characteristics of Explosion Hazards in Methane–Air Mixtures Diluted by Hydrogen

Jiajia Liu <sup>1</sup>, Danyang Yu <sup>1</sup>, Ping Li <sup>1,2,\*</sup>, Xuxu Sun <sup>1,\*</sup> and Xianfeng Chen <sup>1</sup>

<sup>1</sup> School of Safety Science and Emergency Management, Wuhan University of Technology, Wuhan 430070, China

<sup>2</sup> Hubei Key Laboratory of Fuel Cell, Wuhan University of Technology, Wuhan 430070, China

\* Correspondence: vera53@whut.edu.cn (P.L.); xuxusun@whut.edu.cn (X.S.)

**Abstract:** The combustion efficiency of methane can be effectively enhanced with the occurrence of hydrogen. However, the combustion characteristic of premixed methane/hydrogen/air is not fully understood. In this study, the effect of the amount of hydrogen addition on the explosion risk of premixed CH<sub>4</sub>/air combustion was fully investigated through experiments and simulations. The explosion overpressure of premixed CH<sub>4</sub>/air combustion with various hydrogen additions was measured in a standard 20 L spherical closed vessel. Meanwhile, the microscopic flame structures for the same cases were simulated using 2022 Chemkin-Pro software. The results showed that hydrogen could increase the explosion risks of premixed CH<sub>4</sub>/air combustion. The rate of key elementary reactions R38: H + O<sub>2</sub> <=> O + OH and R84: OH + H<sub>2</sub> <=> H + H<sub>2</sub>O in the system could be accelerated by hydrogen. The peak explosion overpressure in the closed chamber is boosted and the arrival time of peak overpressure rise rate is shortened, which raises the danger. Especially under lean and rich combustion conditions, hydrogen could potentially lead to more dangerous situations. With the increase in hydrogen concentration, the reaction rate of key elementary reactions accelerates faster, the peak explosion overpressure increases more, and the peak overpressure rise rate arrives earlier.

**Keywords:** methane; explosive hazards; overpressure; laminar burning velocity



**Citation:** Liu, J.; Yu, D.; Li, P.; Sun, X.; Chen, X. Characteristics of Explosion Hazards in Methane–Air Mixtures Diluted by Hydrogen. *Energies* **2023**, *16*, 6416. <https://doi.org/10.3390/en16186416>

Academic Editor: Bjørn H. Hjertager

Received: 5 July 2023

Revised: 25 August 2023

Accepted: 30 August 2023

Published: 5 September 2023



**Copyright:** © 2023 by the authors. Licensee MDPI, Basel, Switzerland. This article is an open access article distributed under the terms and conditions of the Creative Commons Attribution (CC BY) license (<https://creativecommons.org/licenses/by/4.0/>).

## 1. Introduction

For a considerable period of time, fossil fuels have served as the primary energy source for human production and daily life [1]. Among them, natural gas, as a cleaner alternative to traditional fossil fuels such as coal and oil, has been increasingly popular in the global energy market and widely used in industrial production and residential applications [2,3]. The main component of natural gas is methane, which is one of the primary gas fuels for industrial and domestic purposes. It is an excellent alternative energy source and generates the lowest amount of carbon dioxide among the three common fossil fuels [4,5]. However, with the continuous advancement of human society and the growing global demand for energy, the development and utilization of sources have led to the rapid depletion of limited fossil fuel reserves worldwide and increasing environmental pollution problems. Consequently, it is urgent to explore and utilize new alternative fuels (especially renewable fuels) to provide cleaner, more efficient, and higher thermal efficiency combustion [6–11].

Compared with traditional fossil energy, hydrogen, as a new type of high-energy source, possesses numerous advantages, including non-pollution, low ignition energy, wide flammability limits, high efficiency, renewability, and environmental protection. It has attracted increasing attention in the global energy market and plays a crucial role in addressing the fossil fuel crisis and mitigating climate change [8,12]. With the development of science and technology, hydrogen energy has been widely used in various fields, such as transportation, industry, energy storage equipment, and aerospace. Hydrogen fuel cell vehicles are zero-emission vehicles, which have become an important development

direction in the global transportation field. Hydrogen energy can be used in industrial processes such as the preparation of chemicals, synthetic ammonia, and oil refining, as well as in industries such as metal processing and glass manufacturing. Home energy storage devices can use hydrogen energy to store renewable energy such as solar or wind power. For example, magnesium hydride ( $MgH_2$ ) satisfies most of the requisites for a viable hydrogen storage material for mobile as well as stationary applications because of its high storage capacity [13]. Hydrogen energy is also used in aerospace, such as satellites and rockets [14]. At present, the global hydrogen energy industry has entered a stage of rapid development. Governments and enterprises in various countries have increased investment and research to promote the development and application of hydrogen energy technology. Researchers have discovered that blending hydrogen gas into natural gas as a fuel can effectively address issues such as high ignition energy, local flame extinguishment, low power output, slow flame speed, and incomplete combustion [9], and significantly improve flame kinetics and combustion efficiency. However, hydrogen utilization is a double-edged sword. Due to its extremely low ignition energy, wide explosive limits, and higher laminar burning velocity, the explosion risk of hydrogen gas is much higher than other hydrocarbon fuels [10,15,16], there are many safety problems in the application of hydrogen energy, such as hydrogen embrittlement [13] and detonation. The intense pressure, high temperature, and strong shockwaves generated during methane and hydrogen gas explosions can cause severe casualties and property damage [17], while their fuel mixtures will inevitably have different ignition and combustion characteristics, posing significant safety hazards in the production, use, storage, and transportation processes of hydrogen-blended fuels [18–21]. The fuel mixture of hydrogen and methane is known as hythane, which is expected to become an alternative clean energy source. To ensure the safe and efficient utilization of hydrogen-rich natural gas (HNG) as a new energy source, it is essential to explore the fundamental phenomena and combustion characteristics during the combustion and explosion processes of methane–hydrogen mixtures [20]. Currently, numerous scholars at home and abroad have conducted extensive research on the combustion characteristics of methane, hydrogen, and methane–hydrogen mixtures.

The explosion pressure is one of the important parameters of concern in the assessment of combustible gas explosion risks. Previous researchers have conducted a series of studies on the explosion pressure of methane, hydrogen, and their mixtures in different containers, and the collective findings consistently demonstrate that adding hydrogen to methane increases the explosion pressure of the gas mixture. Qiangqiang Hao [20] and S.D. Emami [21] conducted experiments in different containers, and they both found that, especially in the lean condition, the addition of hydrogen significantly enhanced the explosion intensity of the premixed gas, which was manifested by an increase in the explosion pressure and pressure rise rate, and a decrease in combustion time. Yanchao Li [22] discovered that under lean and stoichiometric conditions, flame instability could be attributed to the combined effects of diffusion heat and fluid dynamic instability, which were enhanced with an increase in hydrogen addition. While under rich condition, flame instability was attributed to the competing effects of the above two factors. Qiuju Ma [23] observed that the experimental values of the peak overpressure were lower than the adiabatic ones due to heat loss. And the explosion pressure and temperature under adiabatic conditions showed a slight decrease with the addition of hydrogen. The positive effect of hydrogen addition on  $(dp/dt)_{max}$  at higher hydrogen concentrations was much more pronounced than the one at lower hydrogen concentrations.

The laminar burning velocity is one of the key parameters determining the combustion characteristics of a mixture, which is closely related to many complex phenomena during flame propagation, such as flame stability and flame height. Recently, some experimental and numerical studies reported the measurement of laminar burning velocity for the methane–hydrogen–air flames [24–27] and found that an increase in hydrogen content led to a significant reduction in the critical radius and Markstein length, indicating that the addition of hydrogen enhanced both diffusion thermal instability and fluid dynamic

instability, so as to increase the laminar burning velocity of methane–hydrogen–air flames. The laminar burning velocity of the blends was always lower than those obtained by averaging the laminar burning velocities of the pure fuels according to their molar proportions. Akihiro Ueda [28] used the spherical expanding flame method to measure the laminar burning velocity of mixtures containing hydrogen, methane, carbon dioxide, and air. The results revealed that as the mole fraction of  $\text{CO}_2$  increased, the laminar burning velocity decreased, while it increased with the addition of hydrogen. These trends can be attributed to variations in the thermal diffusivity of the mixture, which increases with hydrogen addition and decreases with carbon dioxide dilution.

Currently, the chemical kinetic mechanisms of methane and hydrogen have been reasonably well understood. However, when methane and hydrogen are mixed, they can exhibit distinct behaviors. Chemical reaction kinetics simulations and detailed reaction mechanisms were employed to analyze the impact of hydrogen addition on the chemical kinetics of methane–air flames. Fei Ren [29] and Erjiang Hu [30] utilized the Chemkin II/Premix program, incorporating detailed chemical reaction mechanisms from GRI Mech 3.0 to analyze the sensitivity and flame structure of methane–hydrogen–air flames under different initial temperatures, pressures, and hydrogen contents. They found that the laminar burning velocity depends on the competition between the main chain branching reaction and the chain recombination reaction. The overall suppression (or enhancement) of the chemical reaction with the increase in initial pressure (or temperature) is closely related to the decrease (or increase) of H, O, and OH mole fractions in the flames. Jinhua Wang [31] found that when the hydrogen content exceeded 20%, the role of  $\text{H}_2$  in the flame transitioned from an intermediate species to a reactant.

Based on the above studies, it can be concluded that research on the characteristics of the combustion of premixed  $\text{CH}_4/\text{H}_2/\text{air}$  can effectively guide the utilization of hydrogen-rich fuels. However, previous studies mostly focused on fuel mixtures with a low-volume fraction of hydrogen addition (up to 40%) and narrow equivalence ratios, resulting in a relative scarcity of fundamental combustion and explosion data and mechanism studies for  $\text{CH}_4/\text{H}_2/\text{air}$ . An in-depth understanding of explosion phenomena and data is necessary for evaluating the hazards of the blend fuel  $\text{CH}_4/\text{H}_2$  energy systems and guiding the design and application of fuel formulations. Therefore, this study aims to investigate the effect and mechanism of hydrogen addition (ranging from 0% to 80% by volume) on the combustion and explosion characteristics of  $\text{CH}_4/\text{H}_2/\text{air}$  mixtures (equivalence ratios ranging from 0.6 to 1.6), so as to provide data and theoretical support for the safe application of HNG.

## 2. Experimental and Numerical Methods

The combustion experiments were carried out in a standard 20 L spherical vessel consisting of the following parts: gas distribution system, ignition device, data acquisition system, and synchronous control system. Figure 1 shows a schematic of the experimental setup.

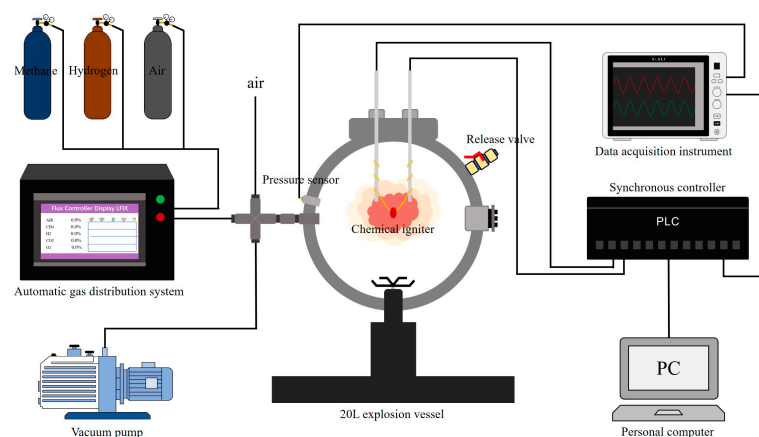


Figure 1. Schematic of the experimental setup.

The gas distribution system includes vacuum pump, automatic gas mixer, and experimental gas cylinders. Firstly, the spherical chamber was evacuated to a vacuum (about 100 Pa) with the vacuum pump, and then the set ratio of premixed CH<sub>4</sub>/H<sub>2</sub>/air was introduced into the spherical chamber through the gas mixer. After 30 s of static settling, the mixture was ignited. In this experiment, the explosion of the gas mixture was triggered by the ignition electrode detonating the chemical ignitor. The composition ratio (mass ratio) of the chemical ignitor is based on GB/T 16,425 and ASTM E1226, which is zirconium powder: barium peroxide: barium nitrate = 4:3:3. The overpressure near the wall of the spherical chamber was collected by a Kistler (Winterthur, Switzerland) 601CA pressure sensor (sensitivity –37 PC/bar, pressure range 0–250 bar), and the overpressure data was recorded and stored by a data acquisition instrument (HIOKI, Nagano, Japan). The ignition and overpressure acquisition were synchronized by a self-designed and manufactured synchronous controller. The purity of methane and hydrogen used in this experiment was both 99.999%, and the air was a synthetic air with a volume fraction of 21% pure oxygen and 79% pure nitrogen, all provided by Wuhan Zhongyixing Chemical Technology Co. (Wuhan, China).

All tests were conducted with initial temperature of 298 K and initial pressure of 0.1 MPa. The equivalence ratio was set to 0.6/0.7/0.8/0.9/1/1.1/1.2/1.3/1.4/1.5/1.6, respectively. Under each equivalence ratio, the volume fraction of hydrogen in the fuel  $x_{H_2}$  was set to 0%/20%/40%/60%/80% respectively. Three repeated tests were conducted for the same case and in total 165 tests were carried out in our study.

The equivalence ratio ( $\Phi$ ) of the mixture is defined as

$$\Phi = \frac{F/A}{(F/A)_{st}} \quad (1)$$

where  $(F/A)$  refers to the fuel–air ratio, and  $(F/A)_{st}$  is the stoichiometric value of  $(F/A)$ , which is the molar ratio between the reactants and products calculated from the chemical reaction metrology equation.  $\Phi < 1$  is for lean fuel,  $\Phi = 1$  is for stoichiometric fuel, and  $\Phi > 1$  is for rich fuel.

The hydrogen addition (volume fraction of hydrogen) in the mixture is defined as

$$x_{H_2} = \frac{V_{H_2}}{V_{H_2} + V_{CH_4}} \quad (2)$$

where the  $x_{H_2}$  is volume fraction of hydrogen,  $V_{H_2}$  is hydrogen volume,  $V_{CH_4}$  is methane volume.

Chemkin-Pro software is a powerful package for solving complex chemical reaction problems, commonly used for simulating combustion processes, catalytic processes, chemical vapor deposition, plasma, and other chemical reactions. It is capable of simulating complex chemical reactions using various chemical reaction mechanism models and can perform rapid and accurate kinetic analysis of reactions [32]. This software has been used and verified by many researchers [29–31]. In this work, Ansys 2022 Chemkin-Pro was used to simulate the combustion process and calculate the laminar flame speed of premixed CH<sub>4</sub>/H<sub>2</sub>/air. The most recent version of Chemkin-Pro commercial-quality software is a product of evaluation from combustion kinetics code Chemkin II developed at Scandia National Laboratories, currently held by Reaction Design (US Company, San Diego, CA, USA) [33].

The chemical reaction mechanism used in this study was GRI-Mech 3.0 [34], which can simulate the combustion process of low hydrocarbon fuels, including related rate coefficient expressions and thermochemical parameters of 325 elementary reactions and 53 species. The GRI-Mech 3.0 mechanism was validated by extensive experimental data for methane, ethane, carbon monoxide, and hydrogen [35–37].

### 3. Results and Discussion

#### 3.1. Experimental Results

Figure 2 shows the curves of typical overpressure and the pressure rise rate over time during the combustion of  $\text{CH}_4/\text{H}_2/\text{air}$  in the spherical chamber. The equivalence ratio of the premixed  $\text{CH}_4/\text{H}_2/\text{air}$  is 1.0 and the volume fraction of hydrogen in the fuel  $x_{\text{H}_2}$  is 20%. Shortly after the premixed gas is ignited at the center of the closed space, a fireball is formed and the unburned gas moves outward due to the thermal expansion of the combustion products, which leads to the formation of a flame front and a combustion pressure wave propagating in all directions. Since the propagation velocity of the combustion pressure wave is faster than that of the flame front, the combustion pressure wave reaches the chamber wall first and strikes the pressure sensor to generate a pressure signal. During the laminar combustion process in the initial stage of the reaction, the combustion speed is slow, and the overpressure of the combustion wave is small [38]. As shown in Figure 2, the overpressure and the overpressure rise rate increase slowly during the initial reaction period of 0 to  $t_1$  ms. With the influence of fluid dynamic instability (Darrieus–Landau), thermal diffusion instability (Rayleigh–Taylor instability) [12,39], etc., the combustion speed gradually increases, and turbulent combustion occurs. The overpressure strength increases rapidly until it reaches the peak overpressure,  $P_{\text{max}}$ , at time,  $t_3$ . After that, the chamber pressure gradually decreases due to the consumption of fuel and wall heat loss. The peak overpressure ( $P_{\text{max}}$ ) is related to the flame propagation speed and the chemical reaction heat effect, which is an important indicator to measure the explosion hazard of premixed flammable gas combustion. In addition, the overpressure rise rate ( $dp/dt$ ) of the flammable gas, which is calculated from the measured pressure time history on the wall, is another important indicator. That is, within the same amount of time, a higher overpressure rise rate represents a greater destructive power of the explosion. So, the time when the peak of the overpressure rise rate ( $dp/dt_{\text{max}}$ ) arrives represents the most dangerous moment ( $t = t_2$ , as shown in Figure 2). In this study,  $t_{\text{danger}}$  is defined as the duration time from ignition to the most dangerous moment for each case, which is the exact moment the peak of overpressure rise rate occurs.

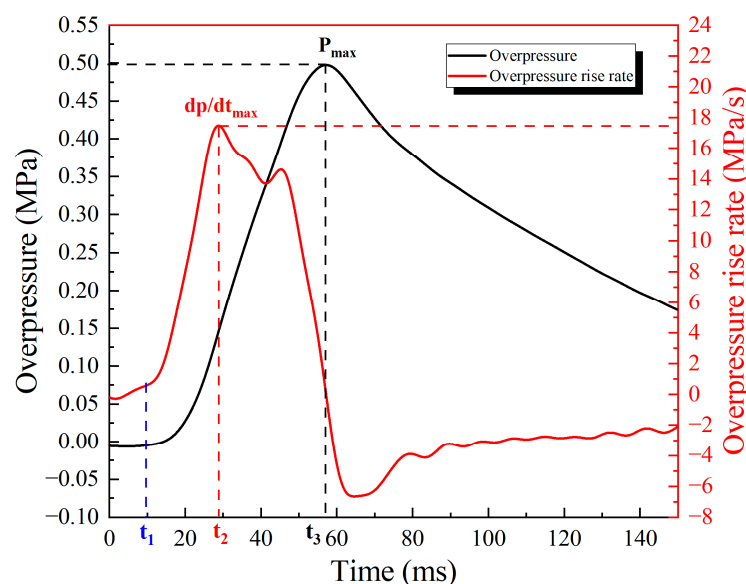


**Figure 2.** Typical time history of overpressure and overpressure rising rate during combustion of premixed  $\text{CH}_4/\text{H}_2/\text{air}$  inside vessel ( $\Phi = 1$ ,  $x_{\text{H}_2} = 20\%$ ).

In order to investigate the effect of hydrogen on the peak overpressure caused by the combustion of premixed  $\text{CH}_4/\text{air}$ , Figure 3 depicts the relationship between the peak overpressure and the equivalence ratio with different hydrogen additions. It can be seen in Figure 3 that the relationships between the peak overpressure induced by different volumes

of hydrogen addition, and the equivalence ratio shows a similar trend. That is, the peak overpressure increases first, then decreases with the increase in equivalence ratio, and the peak overpressure reaches the maximum value near the stoichiometric ratio. In addition, the amount of hydrogen addition also has a significant effect on the peak overpressure. As shown in Figure 3, the black curve without hydrogen addition is below all the other curves, indicating that hydrogen can significantly increase the peak overpressure in the closed vessel. However, the increase amplitude of peak overpressure is different under different hydrogen additions.

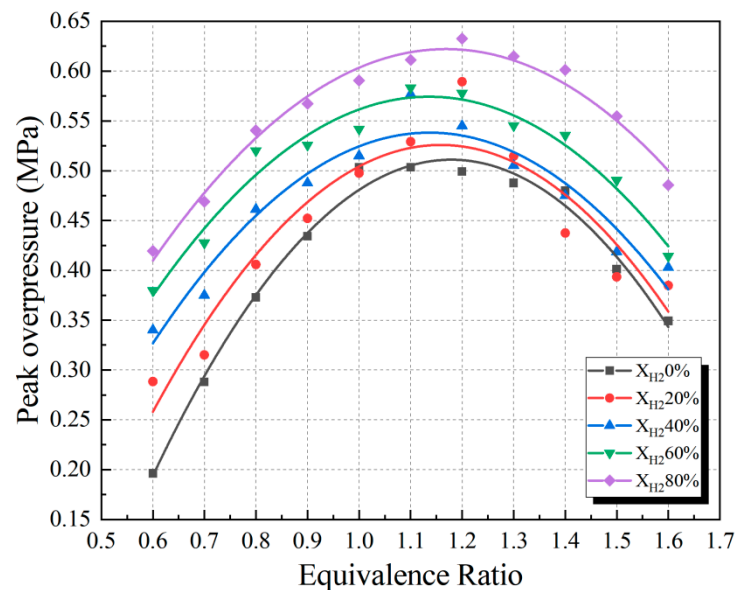


Figure 3. Effect of hydrogen on the peak overpressure at different equivalence ratios.

To further investigate the effect of the amount of hydrogen on the peak overpressure of premixed CH<sub>4</sub>/air combustion, Figure 4 plots the relationships between the hydrogen addition amount and the dimensionless peak overpressure at different equivalence ratios. The dimensionless peak overpressure is defined as the peak overpressure increasing amplitude induced by a specific hydrogen addition compared with that of no hydrogen addition, as follows:

$$\varepsilon = \frac{P_{\max(x_{H_2})} - P_{\max(\text{without } H_2)}}{P_{\max(\text{without } H_2)}} \times 100\% \quad (3)$$

where  $\varepsilon$  is the dimensionless peak overpressure,  $P_{\max(x_{H_2})}$  is the peak overpressure caused by the combustion of premixed CH<sub>4</sub>/H<sub>2</sub>/air with different hydrogen volume fractions  $x_{H_2}$ , and  $P_{\max(\text{without } H_2)}$  is the peak overpressure caused by the combustion of premixed CH<sub>4</sub>/air under different equivalence ratios. An interesting phenomenon can be observed from Figure 4: when the equivalence ratio is near the stoichiometry ( $\Phi = 0.8$ – $1.2$ ), hydrogen does not cause a significant change in the  $\varepsilon$ , as shown in Figure 4a. For example, when the equivalence ratio is  $\Phi = 1.1$  (as shown by the green line in Figure 4a), the peak overpressure generated by the combustion of premixed CH<sub>4</sub>/air is 0.59 MPa, and when the volume fraction of hydrogen addition  $x_{H_2} = 20\%$ , the peak overpressure is 0.66 MPa, resulting in an  $\varepsilon$  of 11.9%. When the amount of hydrogen addition increases to  $x_{H_2} = 80\%$ , the peak overpressure increases to 0.69 MPa, and  $\varepsilon$  just increases to 16.9%. The same phenomenon is observed only when the hydrogen addition  $x_{H_2} < 40\%$  in lean ( $\Phi = 0.6$ – $0.7$ ) and rich ( $\Phi = 1.3$ – $1.6$ ) conditions. However, when the volume fraction of hydrogen addition  $x_{H_2} > 40\%$ ,  $\varepsilon$  increases rapidly with the increase in the hydrogen addition. As shown in Figure 4b, when the volume fraction of hydrogen  $x_{H_2} = 20\%$ , the  $\varepsilon$  is 38% and 8%, with the equivalence ratios  $\Phi$  as 0.6 and 1.6, respectively. When adding more hydrogen to premixed CH<sub>4</sub>/air with  $x_{H_2} = 40\%$ , the  $\varepsilon$  is still 38% and 8%, respectively. However, when

the volume fraction of hydrogen addition increases to  $x_{H_2} = 60\%$ , the  $\varepsilon$  rapidly rises to 69% and 27%, respectively.

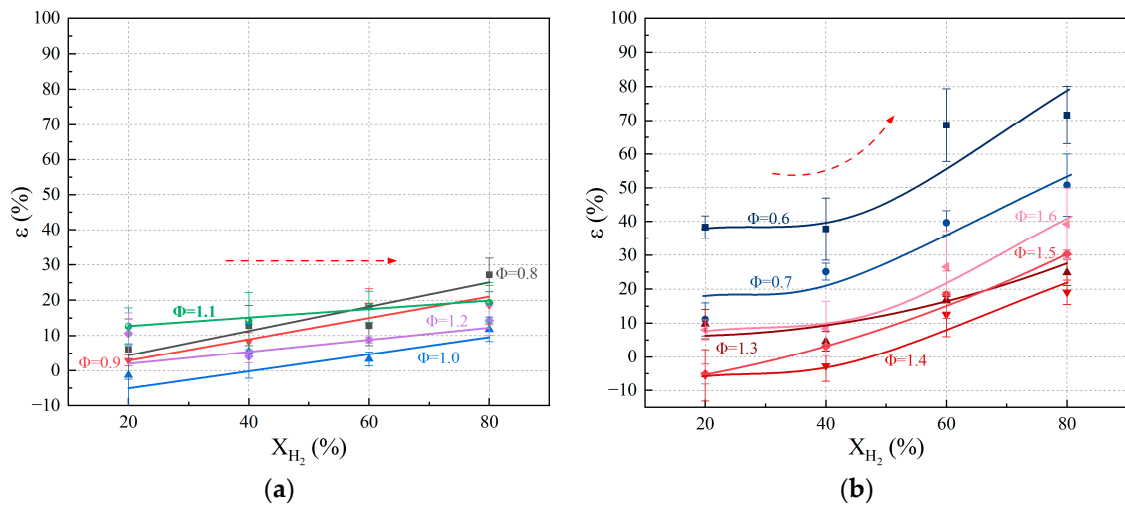


**Figure 4.** Effect of hydrogen amount on the dimensionless of peak overpressure rise rate at different equivalence ratios. (a) Moderate ratios; (b) Lean and rich conditions.

Figure 5 shows the variations of the most dangerous time  $t_{danger}$  along with the different equivalent ratios. In general, the red line ( $x_{H_2} = 0\%$ ) is above the other lines in Figure 5, indicating that the addition of hydrogen can shorten the time to reach the peak overpressure rise rate, that is, the dangerous moment is advanced. In addition, at the same equivalent ratio when  $\Phi = 0.8–1.2$ , the amount of hydrogen addition shows no significant influence on the arrival of danger time,  $t_{danger}$ . In contrast, the amount of hydrogen addition plays an important role in the arrival of danger time,  $t_{danger}$ , under lean ( $\Phi = 0.6–0.7$ ) and rich ( $\Phi = 1.3–1.6$ ) conditions, as shown in the dashed box in Figure 5. That is, the appearance of hydrogen in the combustion of premixed  $CH_4$ /air could increase the combustion explosion overpressure and shorten the arrival time of danger, which enhances the combustion explosion hazard. Moreover, under lean ( $\Phi = 0.6–0.7$ ) and rich ( $\Phi = 1.3–1.6$ ) conditions, the amount of hydrogen addition also affects the combustion overpressure and  $t_{danger}$ .

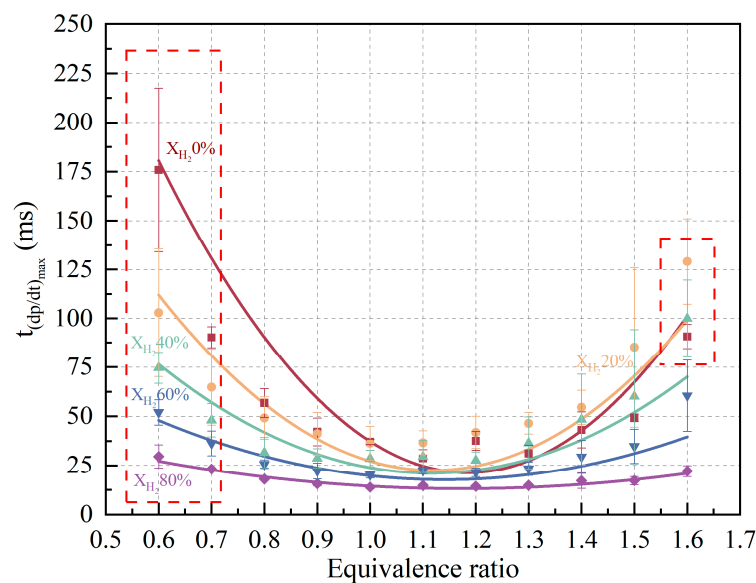


**Figure 5.** The variations of the most dangerous time,  $t_{danger}$ , along with the different equivalent ratios.

### 3.2. Effect of Hydrogen on the Peak Overpressure and Arrival Time of the Dangerous Moment of Premixed CH<sub>4</sub>/Air Combustion

Figure 6 shows the relationships between the laminar burning velocity and equivalence ratio for premixed CH<sub>4</sub>/H<sub>2</sub>/air at different hydrogen addition ratios. The solid line represents the simulation results obtained through Chemkin-Pro, and experimental laminar burning velocities by Xiaobo Shen [40], Sven Eckart [41], K.J. Bosschaart [42], R.T.E. Hermanns [43], Hu [44], Xiao Cai [45], Elna J.K. Nilsson [46] are also shown in Figure 6. It can be seen from Figure 6 that the deviation between experimental data and the simulation is small, indicating that GRI-Mech 3.0 can be used for the simulation calculation of premixed CH<sub>4</sub>/H<sub>2</sub>/air laminar combustion. In addition, it can be seen in Figure 6 that regardless of the amount of hydrogen addition, the laminar burning velocity shows a similar trend: it increases first and then decreases with increasing equivalence ratio, reaching a peak near stoichiometry. Moreover, the black curve without hydrogen addition is below all other curves, indicating that the addition of hydrogen significantly improves the laminar burning velocity of the combustion of premixed CH<sub>4</sub>/air. For a certain equivalence ratio, the amount of methane would reduce if the amount of hydrogen increases. Since the combustion heat of hydrogen is greater than that of methane, the peak overpressure produced by combustion with more hydrogen is larger, and the time to reach the dangerous moment is shorter, which is consistent with the experimental phenomenon observed in Section 3.1.

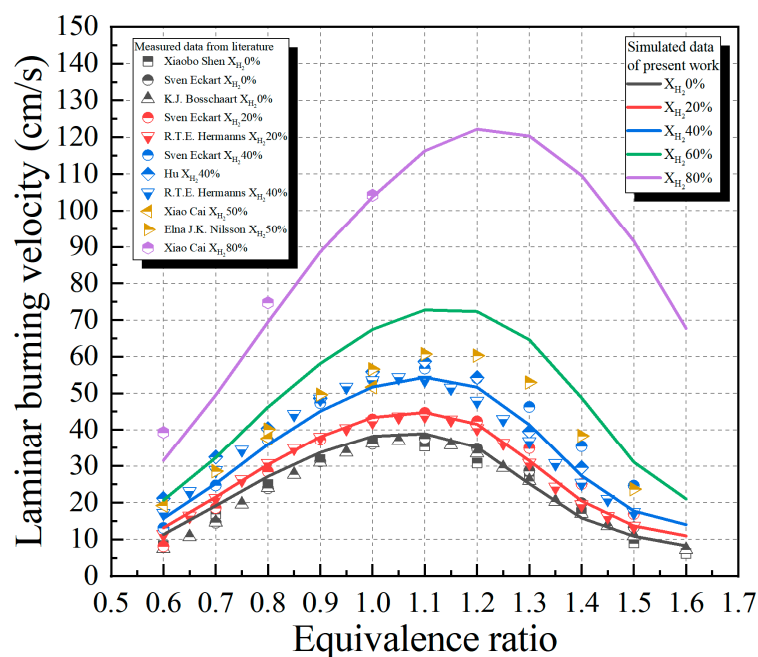


**Figure 6.** Laminar burning velocity versus equivalence ratios for premixed CH<sub>4</sub>/H<sub>2</sub>/air with different volume fractions of hydrogen.

The combustion velocities of carbon–hydrogen compounds are mainly affected by chain branching and chain growth reactions involving key radicals such as H, O, and OH. The main elementary reactions associated with H, O, and OH radicals during the combustion process of premixed CH<sub>4</sub>/H<sub>2</sub>/air are R38: H + O<sub>2</sub> ⇌ O + OH and R84: OH + H<sub>2</sub> ⇌ H + H<sub>2</sub>O. To further investigate the effect of hydrogen addition on premixed CH<sub>4</sub>/air combustion, Figure 7 plots the effect of the amount of hydrogen addition on the reaction rates of elementary reactions R38 and R84 at different equivalence ratios. The rate of production (ROP) represents reaction intensity at different times. It can be seen in Figure 7 that at all equivalence ratio conditions, the appearance of hydrogen significantly advances both the elementary reactions R38 and R84 and accelerates the two reactions with a higher peak rate of production. For example, when hydrogen is not added (black line), the peak rate of production for R84 occurs at 5.44 mm, 5.17 mm, and 5.74 mm when equivalent

ratios  $\Phi = 0.6$ ,  $\Phi = 1$ ,  $\Phi = 1.6$  as shown in Figure 7a–c, respectively. And the corresponding peak reaction rates of productions are  $3.42 \times 10^{-4} \text{ mol/cm}^3 \cdot \text{s}$ ,  $58.5 \times 10^{-4} \text{ mol/cm}^3 \cdot \text{s}$ , and  $5.82 \times 10^{-4} \text{ mol/cm}^3 \cdot \text{s}$ . When volume fraction of the hydrogen addition is  $x_{H_2} = 80\%$  (orange line), the R84 occurs at 5.15 mm, 5.06 mm, and 5.15 mm, and the corresponding peak reaction rate of productions are  $48.9 \times 10^{-4} \text{ mol/cm}^3 \cdot \text{s}$ ,  $396 \times 10^{-4} \text{ mol/cm}^3 \cdot \text{s}$ , and  $219 \times 10^{-4} \text{ mol/cm}^3 \cdot \text{s}$ , respectively.

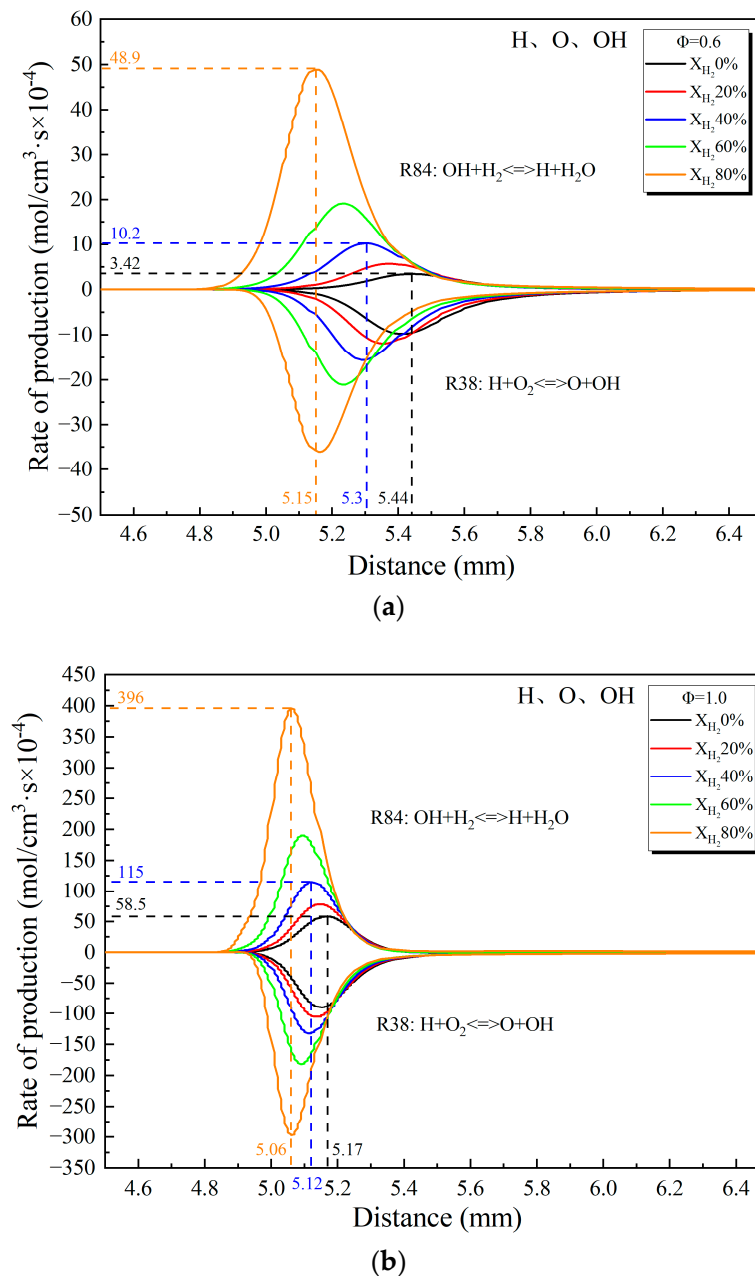
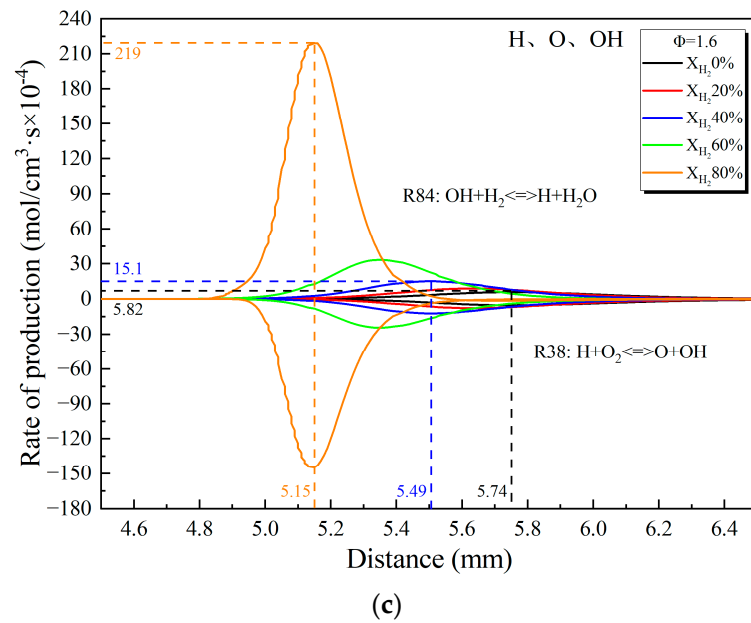
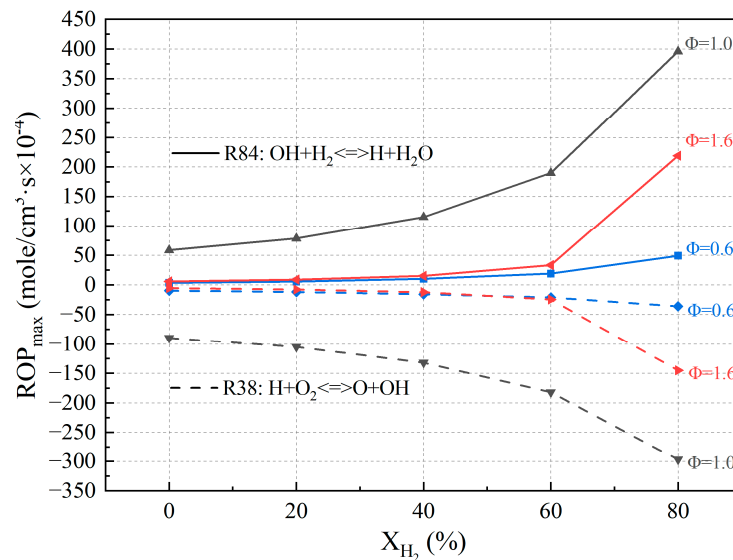


Figure 7. Cont.



**Figure 7.** Effect of hydrogen addition content on the reaction rates of major radicals at different equivalence ratios. (a)  $\Phi = 0.6$ , (b)  $\Phi = 1.0$ , (c)  $\Phi = 1.6$ .

A high peak rate of production ( $ROP_{max}$ ) corresponds to a vigorous reaction. Figure 8 plots the variation of the peak reaction rates of production ( $ROP_{max}$ ) for key elementary reactions R38 and R84 along with different hydrogen volume fractions,  $x_{H_2}$ . It can be seen from Figure 8 that under all equivalence ratios, the  $ROP_{max}$  of the two reactions increases as the amount of hydrogen addition increases. It can be inferred that the reaction becomes more intense with increasing hydrogen addition. That is, hydrogen accelerates elementary reactions R38 and R84 so as to increase the laminar burning velocity of premixed  $CH_4/H_2/air$  combustion, thereby increasing the peak overpressure and the pressure rise rate, as observed in Section 3.1.



**Figure 8.** Variations in the peak reaction rates of production ( $ROP_{max}$ ) for key elementary reactions R38 and R84 along with different hydrogen volume fractions.

### 3.3. Effect of Hydrogen on Explosion Hazards under Lean and Rich Combustion Conditions

Next, we further discuss the reason that an increasing amount of hydrogen addition leads to increasing explosion risk of premixed  $CH_4/air$  combustion under lean and rich

conditions. The peak rate of production ( $ROP_{max}$ ) is selected to represent the degree of possible explosion risk. In order to explore the effect of amount of hydrogen addition on  $ROP_{max}$ , the dimensionless  $ROP_{max}$  is calculated as follows:

$$\gamma = \frac{ROP_{max(x_{H_2})} - ROP_{max(without H_2)}}{ROP_{max(without H_2)}} \times 100\% \quad (4)$$

where  $\gamma$  is the dimensionless peak ROP,  $ROP_{max(x_{H_2})}$  is the peak ROP caused by the combustion of premixed  $CH_4/H_2/air$  with different hydrogen volume fractions,  $x_{H_2}$ , and  $ROP_{max(without H_2)}$  is the peak ROP caused by combustion of premixed  $CH_4/air$  under different equivalence ratios. Figure 9 shows the relationships between the dimensionless  $ROP_{max}$  for the key elementary reaction R84 and the amount of hydrogen addition at different equivalence ratios. It is shown in Figure 9 that the dimensionless  $ROP_{max}$  is 0.97% when hydrogen volume fraction  $X_{H_2} = 20\%$  under the equivalent ratio of  $\phi = 1$ . When adding more hydrogen,  $X_{H_2} = 80\%$ , to the premixed  $CH_4/H_2/air$  combustion system under the same case,  $\phi = 1$ , the dimensionless  $ROP_{max}$  just slightly raises to 5.77%. So, it can be inferred that the amount of hydrogen addition has no significant impacts on the dimensionless  $ROP_{max}$  near the stoichiometric ratio ( $\Phi = 1.0$ ). However, under lean ( $\Phi = 0.6$ ) and rich ( $\Phi = 1.6$ ) conditions, the dimensionless  $ROP_{max}$  for key elementary reactions R84 increases significantly with increasing amount of hydrogen addition, as shown in Figure 9, especially when the volume fraction of hydrogen  $X_{H_2} > 40\%$ . For example, in the case of the lean condition ( $\phi = 0.6$ ), the dimensionless  $ROP_{max}$  increases rapidly from 0.66%, 1.98%, to 13.30% when the volume fractions of hydrogen addition are  $X_{H_2} = 20\%/40\%/80\%$ , respectively. That is, compared with the condition of the near stoichiometric ratio, hydrogen presents a greater influence in accelerating the elementary reactions under rich and lean conditions. This leads to the observation of Section 3.1 that the peak overpressure is stronger and the arrival time of the peak overpressure rise rate is shorter. As a result, it exhibits a greater hazard under such circumstances.

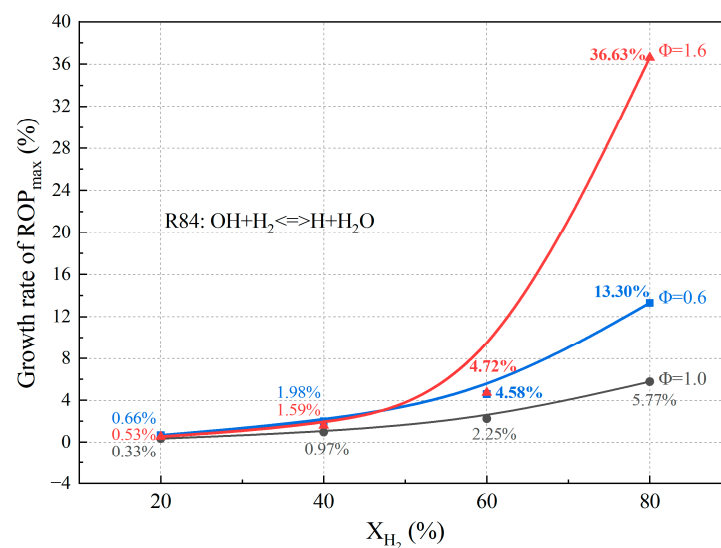


**Figure 9.** Relationships between the dimensionless  $ROP_{max}$  for the key elementary reactions R84 and the amount of hydrogen addition at different equivalence ratios.

#### 4. Conclusions

In this study, the effect of hydrogen addition on the explosion risk of premixed  $CH_4/air$  was investigated from both macroscopic and microscopic perspectives, respectively. The standard 20 L spherical closed vessel experiment was used to measure the explosion overpressure of premixed  $CH_4/H_2/air$  combustion, while the 2022 Chemkin-Pro software was used to calculate the microstructure of the premixed laminar flame. The study found

that hydrogen accelerates elementary reactions R38 and R84 so as to increase the laminar burning velocity of premixed CH<sub>4</sub>/H<sub>2</sub>/air combustion, thereby increasing the peak overpressure and the overpressure rise rate, shortening the arrival time of peak overpressure rise rate, which raises the explosion risk. As the amount of hydrogen addition increases, the rate of production of elementary reactions increases, leading to a higher peak overpressure and a shorter arrival time of the peak overpressure rise rate. In addition, compared with the stoichiometric conditions, hydrogen presents a greater influence under lean and rich conditions, which is attributed to the fact that adding hydrogen substantially increases the rate of production of certain reactions.

**Author Contributions:** Conceptualization, P.L. and X.C.; validation, J.L. and X.S.; formal analysis, J.L. and D.Y.; investigation, J.L., D.Y. and X.S.; writing—original draft preparation, J.L.; writing—review and editing, P.L. and X.C.; supervision, P.L. All authors have read and agreed to the published version of the manuscript.

**Funding:** This research received no external funding.

**Data Availability Statement:** The authors confirm that the data supporting the findings of this study are available within the article.

**Acknowledgments:** This work was supported by Hubei Province unveiling project (No. 2022BEC024); the Fundamental Research Funds for the Central Universities (No. 2022IVA085); and the National Key R&D Program of China (No. 2021YFB4000901).

**Conflicts of Interest:** The authors declare no conflict of interest.

## References

1. Zhao, T.; Chen, X.; Cheng, F.; Lu, K.; Shi, X.; Yu, W. Study on the synergistic inhibition mechanism of multicomponent powders on methane explosions. *Powder Technol.* **2023**, *418*, 118326. [[CrossRef](#)]
2. Mitu, M.; Razus, D.; Schroeder, V. Laminar Burning Velocities of Hydrogen-Blended Methane–Air and Natural Gas–Air Mixtures, Calculated from the Early Stage of p(t) Records in a Spherical Vessel. *Energies* **2021**, *14*, 7556. [[CrossRef](#)]
3. Liu, A.; Lu, X.; Zhou, X.; Xu, C.; Liang, X.; Xiong, K. Experimental investigation on suppression of methane explosion using KHCO<sub>3</sub>/zeolite composite powder. *Powder Technol.* **2023**, *415*, 118157. [[CrossRef](#)]
4. Zhao, T.; Chen, X.; Luo, Z.; Cheng, F.; Lu, K.; Shi, X.; Yu, W. Effect of N<sub>2</sub> inerting on the inhibition of methane explosions by a multicomponent powder. *Fuel* **2023**, *337*, 127203. [[CrossRef](#)]
5. Zhang, X.-H.; Dou, K.; Luo, Z.-M.; Cheng, F.-M.; Xue, H.-L. Kinetic model of methane explosion in a spheroidal explosion tank. *IOP Conf. Ser. Earth Environ. Sci.* **2021**, *647*, 012039. [[CrossRef](#)]
6. Dong, W.; Hu, J.; Xiang, L.; Chu, H.; Li, Z. Numerical Investigation on Combustion Characteristics of Laminar Premixed n-Heptane/Hydrogen/Air Flames at Elevated Pressure. *Energy Fuels* **2020**, *34*, 14768–14775. [[CrossRef](#)]
7. Sun, Z.-Y.; Li, G.-X. Turbulence influence on explosion characteristics of stoichiometric and rich hydrogen/air mixtures in a spherical closed vessel. *Energy Convers. Manag.* **2017**, *149*, 526–535. [[CrossRef](#)]
8. Wang, D.; Ji, C.; Wang, S.; Yang, J.; Tang, C. Experimental investigation on near wall ignited lean methane/hydrogen/air flame. *Energy* **2019**, *168*, 1094–1103. [[CrossRef](#)]
9. Chu, H.; Ren, F.; Xiang, L.; Dong, S.; Qiao, F.; Xu, G. Numerical investigation on combustion characteristics of laminar premixed n-heptane/air flames at elevated initial temperature and pressure. *J. Energy Inst.* **2019**, *92*, 1821–1830. [[CrossRef](#)]
10. Shen, X.; Xu, J.; Wen, J.X. Phenomenological characteristics of hydrogen/air premixed flame propagation in closed rectangular channels. *Renew. Energy* **2021**, *174*, 606–615. [[CrossRef](#)]
11. Dai, T.; Zhang, B.; Liu, H. On the explosion characteristics for central and end-wall ignition in hydrogen-air mixtures: A comparative study. *Int. J. Hydrogen Energy* **2021**, *46*, 30861–30869. [[CrossRef](#)]
12. Li, Y.; Bi, M.; Gao, W.; Cong, H.; Li, B. Self-Acceleration and Self-Similarity of Hydrogen–Methane–Air Flame at Elevated Pressure. *Combust. Sci. Technol.* **2019**, *193*, 1005–1021. [[CrossRef](#)]
13. Shahi, R.R.; Tiwari, A.P.; Shaz, M.A.; Srivastava, O.N. Studies on de/rehydrogenation characteristics of nanocrystalline MgH<sub>2</sub> co-catalyzed with Ti, Fe and Ni. *Int. J. Hydrogen Energy* **2013**, *38*, 2778–2784. [[CrossRef](#)]
14. Okolie, J.A.; Patra, B.R.; Mukherjee, A.; Nanda, S.; Dalai, A.K.; Kozinski, J.A. Futuristic applications of hydrogen in energy, biorefining, aerospace, pharmaceuticals and metallurgy. *Int. J. Hydrogen Energy* **2021**, *46*, 8885–8905. [[CrossRef](#)]
15. Zheng, L.; Zhu, X.; Wang, Y.; Li, G.; Yu, S.; Pei, B.; Wang, Y.; Wang, W. Combined effect of ignition position and equivalence ratio on the characteristics of premixed hydrogen/air deflagrations. *Int. J. Hydrogen Energy* **2018**, *43*, 16430–16441. [[CrossRef](#)]
16. Cao, W.; Li, W.; Yu, S.; Zhang, Y.; Shu, C.-M.; Liu, Y.; Luo, J.; Bu, L.; Tan, Y. Explosion venting hazards of temperature effects and pressure characteristics for premixed hydrogen-air mixtures in a spherical container. *Fuel* **2021**, *290*, 120034. [[CrossRef](#)]

17. Zhang, C.; Shen, X.; Wen, J.X.; Xiu, G. The behavior of methane/hydrogen/air premixed flame in a closed channel with inhibition. *Fuel* **2020**, *265*, 116810. [CrossRef]
18. Xiao, H.; Mao, Z.; An, W.; Sun, J. Experimental and LES investigation of flame propagation in a hydrogen/air mixture in a combustion vessel. *Chin. Sci. Bull.* **2014**, *59*, 2496–2504. [CrossRef]
19. Zhang, K.; Luo, T.; Li, Y.; Zhang, T.; Li, X.; Zhang, Z.; Shang, S.; Zhou, Y.; Zhang, C.; Chen, X.; et al. Effect of ignition, initial pressure and temperature on the lower flammability limit of hydrogen/air mixture. *Int. J. Hydrogen Energy* **2022**, *47*, 15107–15119. [CrossRef]
20. Hao, Q.; Luo, Z.; Wang, T.; Xie, C.; Zhang, S.; Bi, M.; Deng, J. The flammability limits and explosion behaviours of hydrogen-enriched methane-air mixtures. *Exp. Therm. Fluid Sci.* **2021**, *126*, 110395. [CrossRef]
21. Emami, S.D.; Rajabi, M.; Hassan, C.R.C.; Hamid, M.D.A.; Kasmani, R.M.; Mazangi, M. Experimental study on premixed hydrogen/air and hydrogen–methane/air mixtures explosion in 90 degree bend pipeline. *Int. J. Hydrogen Energy* **2013**, *38*, 14115–14120. [CrossRef]
22. Li, Y.; Bi, M.; Li, B.; Zhou, Y.; Gao, W. Effects of hydrogen and initial pressure on flame characteristics and explosion pressure of methane/hydrogen fuels. *Fuel* **2018**, *233*, 269–282. [CrossRef]
23. Ma, Q.; Zhang, Q.; Chen, J.; Huang, Y.; Shi, Y. Effects of hydrogen on combustion characteristics of methane in air. *Int. J. Hydrogen Energy* **2014**, *39*, 11291–11298. [CrossRef]
24. Coppens, F.H.V.; De Ruyck, J.; Konnov, A.A. Effects of hydrogen enrichment on adiabatic burning velocity and NO formation in methane+air flames. *Exp. Therm. Fluid Sci.* **2007**, *31*, 437–444. [CrossRef]
25. Di Sarli, V.; Benedetto, A.D. Laminar burning velocity of hydrogen–methane/air premixed flames. *Int. J. Hydrogen Energy* **2007**, *32*, 637–646. [CrossRef]
26. Hu, E.; Huang, Z.; He, J.; Zheng, J.; Miao, H. Measurements of laminar burning velocities and onset of cellular instabilities of methane–hydrogen–air flames at elevated pressures and temperatures. *Int. J. Hydrogen Energy* **2009**, *34*, 5574–5584. [CrossRef]
27. Huang, Z.; Zhang, Y.; Zeng, K.; Liu, B.; Wang, Q.; Jiang, D. Measurements of laminar burning velocities for natural gas–hydrogen–air mixtures. *Combust. Flame* **2006**, *146*, 302–311. [CrossRef]
28. Ueda, A.; Nisida, K.; Matsumura, Y.; Ichikawa, T.; Nakashimada, Y.; Endo, T.; Kim, W. Effects of hydrogen and carbon dioxide on the laminar burning velocities of methane–air mixtures. *J. Energy Inst.* **2021**, *99*, 178–185. [CrossRef]
29. Ren, F.; Chu, H.; Xiang, L.; Han, W.; Gu, M. Effect of hydrogen addition on the laminar premixed combustion characteristics the main components of natural gas. *J. Energy Inst.* **2019**, *92*, 1178–1190. [CrossRef]
30. Hu, E.; Huang, Z.; He, J.; Miao, H. Experimental and numerical study on lean premixed methane–hydrogen–air flames at elevated pressures and temperatures. *Int. J. Hydrogen Energy* **2009**, *34*, 6951–6960. [CrossRef]
31. Wang, J.; Huang, Z.; Tang, C.; Miao, H.; Wang, X. Numerical study of the effect of hydrogen addition on methane–air mixtures combustion. *Int. J. Hydrogen Energy* **2009**, *34*, 1084–1096. [CrossRef]
32. Smith, G.P.; Golden, D.M.; Frenklach, M.; Moriarty, N.W.; Eiteneer, B.; Goldenberg, M.; Bowman, C.T.; Hanson, R.K.; Song, S.; Gardiner, W.C. GRI-Mech 3.0. Available online: <http://combustion.berkeley.edu/gri-mech/version30/text30.html> (accessed on 25 December 2022).
33. Sieradzka, M.; Rajca, P.; Zajemska, M.; Mlonka-Mędrala, A.; Magdziarz, A. Prediction of gaseous products from refuse derived fuel pyrolysis using chemical modelling software—Ansys Chemkin-Pro. *J. Clean. Prod.* **2020**, *248*, 119277. [CrossRef]
34. Bougrine, S.; Richard, S.; Nicolle, A.; Veynante, D. Numerical study of laminar flame properties of diluted methane-hydrogen-air flames at high pressure and temperature using detailed chemistry. *Int. J. Hydrogen Energy* **2011**, *36*, 12035–12047. [CrossRef]
35. Khan, A.R.; Ravi, M.R.; Ray, A. Experimental and chemical kinetic studies of the effect of H<sub>2</sub> enrichment on the laminar burning velocity and flame stability of various multicomponent natural gas blends. *Int. J. Hydrogen Energy* **2019**, *44*, 1192–1212. [CrossRef]
36. Wang, J.; Liang, Y.; Tian, F.; Chen, C. A numerical study on the effect of CO<sub>2</sub> addition for methane explosion reaction kinetics in confined space. *Sci. Rep.* **2021**, *11*, 20733. [CrossRef]
37. Chemkin Overview. Volume 4. 2015. Available online: <https://www.reactiondesign.com/products/chemkin> (accessed on 23 December 2022).
38. Takizawa, K.; Takahashi, A.; Tokuhashi, K.; Kondo, S.; Sekiya, A. Burning velocity measurement of fluorinated compounds by the spherical-vessel method. *Combust. Flame* **2005**, *141*, 298–307. [CrossRef]
39. Zhou, Y.; Li, Y.; Gao, W. Experimental research on unconfined hydrogen explosion of different gas scale and the overpressure prediction method. *Int. J. Hydrogen Energy* **2023**, *48*, 30985–30996. [CrossRef]
40. Shen, X.; Xiu, G.; Wu, S. Experimental study on the explosion characteristics of methane/air mixtures with hydrogen addition. *Appl. Therm. Eng.* **2017**, *120*, 741–747. [CrossRef]
41. Eckart, S.; Pizzuti, L.; Fritsche, C.; Krause, H. Experimental study and proposed power correlation for laminar burning velocity of hydrogen-diluted methane with respect to pressure and temperature variation. *Int. J. Hydrogen Energy* **2022**, *47*, 6334–6348. [CrossRef]
42. Bosschaart, K.J.; de Goey, L.P.H. The laminar burning velocity of flames propagating in mixtures of hydrocarbons and air measured with the heat flux method. *Combust. Flame* **2004**, *136*, 261–269. [CrossRef]
43. Hermanns, R.T.E.; Konnov, A.A.; Bastiaans, R.J.M.; de Goey, L.P.H.; Lucka, K.; Köhne, H. Effects of temperature and composition on the laminar burning velocity of CH<sub>4</sub>+ H<sub>2</sub>+ O<sub>2</sub>+ N<sub>2</sub> flames. *Fuel* **2010**, *89*, 114–121. [CrossRef]

44. Hu, E.; Huang, Z.; He, J.; Jin, C.; Zheng, J. Experimental and numerical study on laminar burning characteristics of premixed methane–hydrogen–air flames. *Int. J. Hydrogen Energy* **2009**, *34*, 4876–4888. [[CrossRef](#)]
45. Cai, X.; Wang, J.; Bian, Z.; Zhao, H.; Zhang, M.; Huang, Z. Self-similar propagation and turbulent burning velocity of CH<sub>4</sub>/H<sub>2</sub>/air expanding flames: Effect of Lewis number. *Combust. Flame* **2020**, *212*, 1–12. [[CrossRef](#)]
46. Nilsson, E.J.K.; van Sprang, A.; Larfeldt, J.; Konnov, A.A. The comparative and combined effects of hydrogen addition on the laminar burning velocities of methane and its blends with ethane and propane. *Fuel* **2017**, *189*, 369–376. [[CrossRef](#)]

**Disclaimer/Publisher’s Note:** The statements, opinions and data contained in all publications are solely those of the individual author(s) and contributor(s) and not of MDPI and/or the editor(s). MDPI and/or the editor(s) disclaim responsibility for any injury to people or property resulting from any ideas, methods, instructions or products referred to in the content.